AUTONOMOUS TOPOGRAPHIC ACTUATING RADAR (ATAR) SENSING DEVICE FOR THE LUNAR SOUTH POLE

Pablo C. Bedolla Ortiz
Project Lead
Dominican University
pbedollaortiz@my.dom.edu

Julio Rodriguez
Project Co-lead
Dominican University
jrodriguez29@my.dom.edu

Lorena Murguia
Project Management Lead
Dominican University
lmurguia@my.dom.edu

Aaron J. Gomez
Systems Engineer
Dominican University
ajimenez4@my.dom.edu

Kacper Rogalski
Researcher
Dominican University
krogalski@my.dom.edu

Gillian Adkins
Project Manager
Dominican University
gadkins@my.dom.edu

Marlon Selvi
Systems Engineer
Dominican University
mselvi@my.dom.edu

Alex N. Alvarez
Systems Engineer
Dominican University
anavarretealvarez@my.dom.edu

Allison Pea
Project Manager
Dominican University
apea@my.dom.edu

Jorge Cano
Systems Engineer
Dominican University
jcano1@my.dom.edu

Kevin Ruiz
Systems Engineer
Dominican University
kruiz1@my.dom.edu

Ariel Rogers
Faculty Lead
Dominican University
arogers2@dom.edu

Sara Quinn
Faculty Member
Dominican University
squinn@dom.edu

Kevin Murphy
Faculty Member
Dominican University
kmurphy4@dom.edu

March 27, 2024

ABSTRACT

The National Aeronautic and Space Administration (NASA) lunar exploration Artemis mission is in search of new ideas for technology to assist with mission science objectives. The NASA MUREP MINDS multi-semester initiative provides funding to Minority Serving Institutions for research projects geared towards the Artemis mission. Defined customer constraints provide a $1,500 budget for the payload to be carried aboard a spacecraft on an Artemis mission. This paper proposes an inert payload to be manually deployed on the moon, carrying two high-speed LiDAR sensors to aid with the Artemis mission's scientific objectives. The collected LiDAR data is intended for use in creating a high-quality topographic map of the landing site. The lunar terrain presents physical difficulties that can be mitigated by analyzing the collected telemetry to investigate the lunar site. The abundance of terrain information can be used to train future lunar landers and rovers, determine potential anomalies, and assist with engineering in-situ science experiments.

Keywords: ATAR, Lunar, LiDAR, Artemis, Autonomous, Topography

Acronyms

ATAR	Autonomous Topographic Actuating Radar
C&DH	Command and Data Handling
CER	Cost Estimating Relationship
DSN	Deep Space Network
I2C	Inter-Integrated Circuit
ISM	Industrial, Scientific, and Medical
LIDAR	Light Detection and Ranging
LRO	Lunar Reconnaissance Orbiter
MUREP	Minority University Research & Education Project
MINDS	MUREP Innovative New Designs for Space
NASA	National Aeronautics and Space Administration
PM	Project Management
POI	Point of Interest
SPM	Solar Power Manager
TCS	Thermal Control Subsystem

Mission Statement

The deployment of an inert LiDAR collection device would provide primary telemetry. The device is positioned in areas of interest to the mission and will continuously capture LiDAR data fused with additional telemetry, such as temperature, average solar power generated, and atmospheric conditions at the site of placement. The Instrument Suite will collect telemetry, which will be processed by the Command and Data Handling (C&DH) subsystem to be packaged and transmitted to the lunar module. It is then received by the Lunar Reconnaissance Orbiter (LRO) to finally be registered by the Deep Space Network (DSN). The collection of LiDAR data for topographic and environmental analysis of the lunar south pole reduces manual labor and aids in the understanding of landing sites for future manned and unmanned expeditions. In search of potentially habitable environments, this paper discusses the use of scientific instrumentation for autonomous monitoring of POIs, requiring minimal human supervision (1).

System Definition

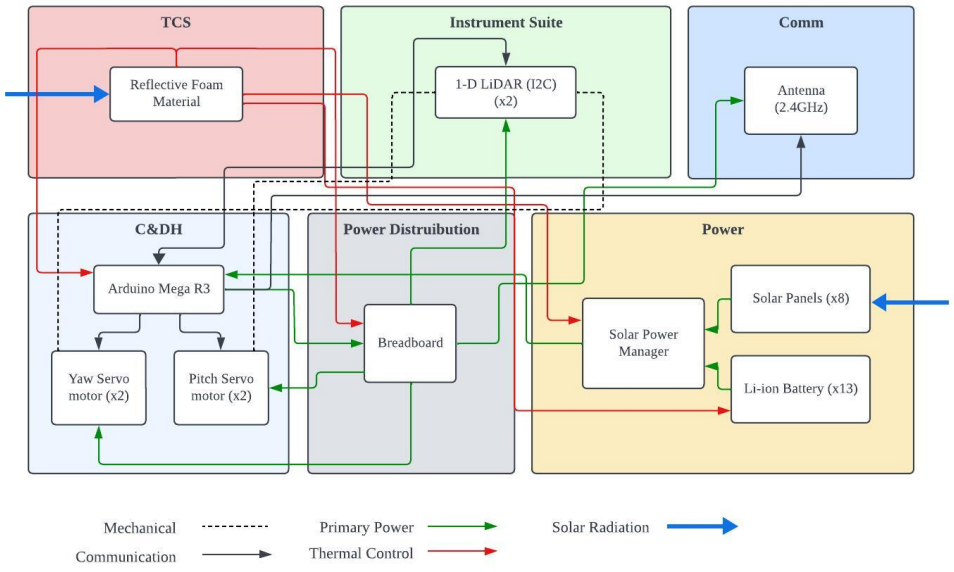

Figure 1: The ATAR functional block diagram delineates TCS, Instrument Suite, Comm, C&DH, internal Power Distribution, and power sources subsystems

Traversing the rough lunar terrain presents a multitude of obstacles for mechanical and payload subsystems. Upon placing the instrument at a POI, the device is faced with freezing-temperatures and must deploy dust mitigation controls. Although not having a mechanical subsystem to mitigate dust intrusion into the instrument, the TCS will carry components to endure the low-temperatures present at the lunar south pole. The Instrument Suite, Communications, Power, and C&DH subsystems are defined as top-level subsystems due to their dependence on lower-level subsystems, which include Thermal Control and Power Distribution subsystems.

System Mass (kg)	2.989
Power Consumption (W/h)	12.17
Design of Life (h)	15.7

Table 1: ATAR instrumentation specifications (6; 7)

Mechanical Subsystem

This paper introduces a device within a shielded body enclosure that houses the Power, Power Distribution, and C&DH subsystems. Spacing between the parallel drip edges provides room for a fitted pan-tilt mechanism chassis setup to mount the LiDAR sensors. The subassembly requires precise positioning to track the pan and tilt angular positions of the LiDAR device in order to visualize the collected data as a 3D point cloud. Figure 2 depicts the coordinate system of the device (2).

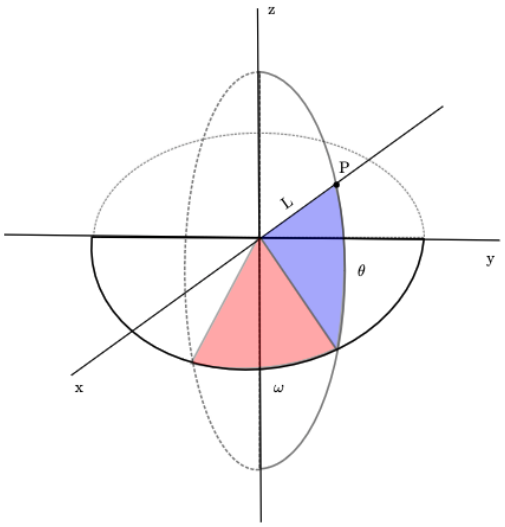

Figure 2: Coordinate system of ATAR scanning positions

The mechanical elements responsible for governing the sensor's sweeping motion are two flat shields housing a rotating turntable. A 180-degree MG90S servomotor (omega) is connected to a small plate above the rotating turntable and below the servo cross, enabling it to adjust the yaw of the system. A 180-degree SG90R servomotor (theta) is connected to a hard plastic alloy bracket, enabling it to adjust the pitch of the system. Two sets of identical two-degree-of-freedom pan-tilt mechanisms are installed at each end of the casing, positioned between both solar arrays. The entire mechanical subsystem provides two degrees of freedom, enabling a complete 360-degree sweep of the surrounding environment.

Placing LiDAR sensors on both ends at the top of the device allows for a complete 360-degree sweep of the environment. Each LiDAR has the ability to perform a 180-degree scan due to the mechanical framework. Together, the pair of LiDAR sensors can perform a full 360-degree scan of the surrounding environment. The Arduino can continuously increment the pitch and yaw of the respective servomotor. The yaw increments 1.8-degrees continuously, collecting data at each angle, until reaching 180-degrees, which is then followed by a 1.8-degree increment in the pitch. The yaw then decrements by 1.8-degrees back to its origin, the pitch then increments by 1.8-degrees again and the process

(a) Head-on View (b) Canted View

Figure 3: CAD model renderings of the servo scanning mechanism used in ATAR

continues until the pitch has reached 180-degrees. The process is reversed when going back to the point of origin of the pitch. A more effective approach to this mechanical system would be deploying a 360-degree LiDAR sensor, removing the need for a second LiDAR. However, the project's funding constraints hindered pursuing this option. This would reduce the payload mass and volume as well as the power consumption, increasing the life expectancy of the system by providing more power for top-level subsystems. This paper provides a mock-up to demonstrate the method of collecting telemetry in dynamic lunar terrains which is common throughout the lunar body.

	Mass (kg)	**Dimensions (mm)**	**Max Power Draw (Wh)**
SG90	0.009	$22.2 \times 11.8 \times 31$	3.5
MG90S	0.0134	$32.5 \times 12 \times 35.5$	1.05

Table 2: Servomotor technical specifications (6; 7)

Power Subsystem

The Power subsystem utilizes solar radiation as a source of continuous energy if available at the selected site. Power is collected through a set of 8 solar panel arrays, all connected in parallel. The power is wired into a Solar Power Manager (SPM) which is designed to receive a nominal voltage of six to twenty-four volts. A set of thirteen lithium-ion batteries is connected in parallel, serving as an alternative power source to the system, through the SPM. The battery power bank serves as a reserve for any excess power that is drawn from the solar panels. A total of 192 watts are preserved for additional power support in the system. All subsystems within the device share and are dependent on the same power source. A nominal power consumption of 12.17 watt hours is projected, yielding a life expectancy of 15.7 hours.

	Mass (kg)	**Dimensions (mm)**	**Max Power Draw (Wh)**
Solar Panels (6V)	0.080	$135 \times 164 \times 1.5$	3.5
21700 Lithium-ion Battery	0.070	70×21.4	14.9

Table 3: Technical specifications for Power subsystem components (10; 9)

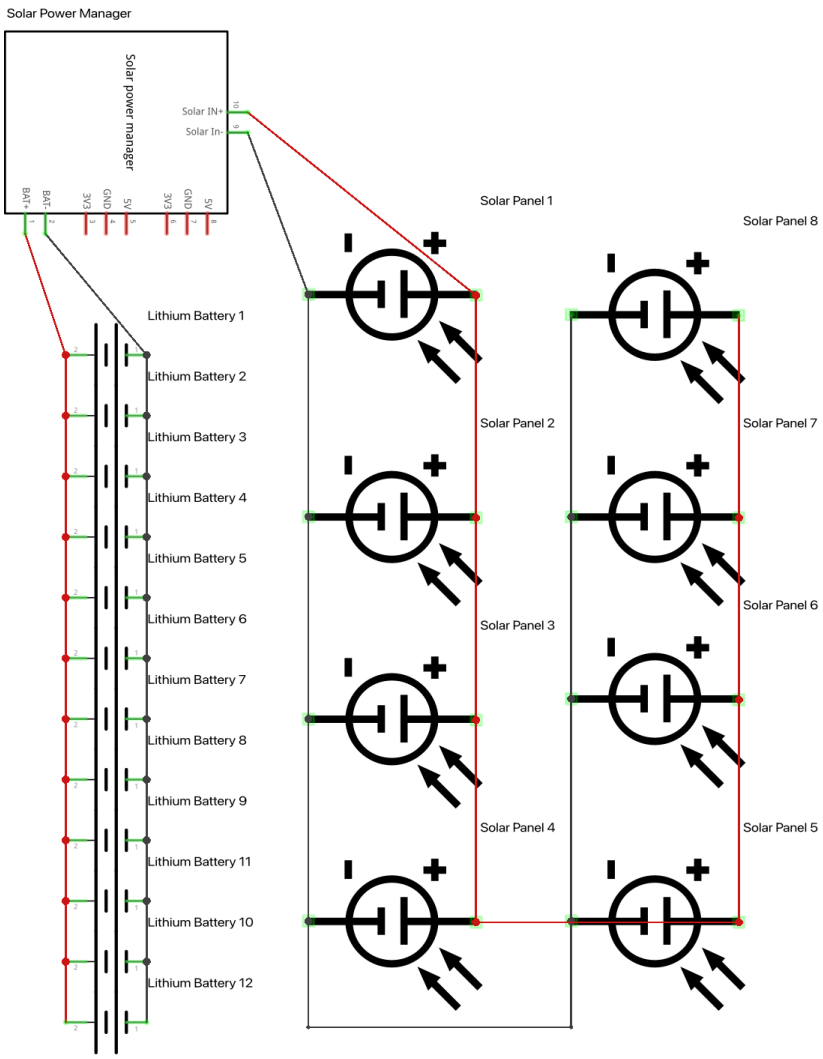

Figure 4: Circuit diagram of ATAR Power subsystem

Power Distribution Subsystem

The Power Distribution subsystem is a network that distributes all power from the Arduino into all necessary subsystem components. The Power Distribution subsystem will only operate if the Power subsystem is receiving enough energy to sustain the subsystem subassemblies. In Figure 5, respective voltages are assigned to connections within the grid, and any additional fields are provided in each subsystem section. If the Power Distribution system receives sufficient power to activate all other interconnected subsystems, it will direct power in the circuit to the respective components. At this juncture in the system, all power flow is managed and distributed.

Thermal Control Subsystem

POIs where the device will be stationed will require that the system endure the freezing lunar south pole(NASA, 2021). The hardware will need to withstand severely low-temperatures, thus requiring efficient thermal control management. Kapton heaters aboard will assist in maintaining operational temperatures for all components to effectively perform their tasks. Reflective foam material is used around the exterior of the device in order to reflect radiation. This will keep the device operational within the expected temperature range, which is typically from 20 to 386K. An effective Thermal Control subsystem is critical to the lifespan and effectiveness of the instrument (3).

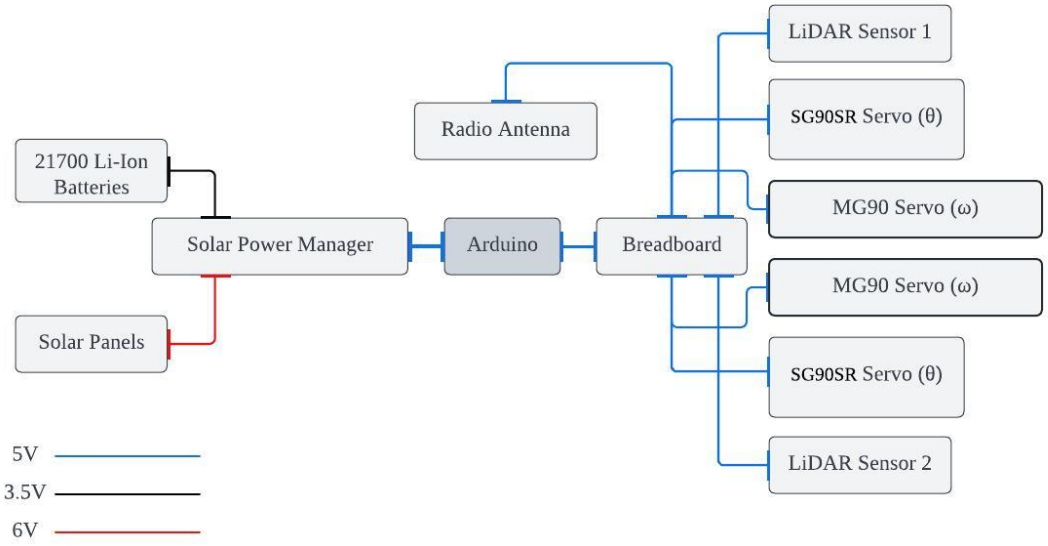

Figure 5: Overview of the ATAR Power Distribution subsystem with voltages assigned to the connections

Command and Data Handling

The Command and Data Handling (C&DH) subsystem employs a microcontroller board, Arduino Mega 2560 Rev3, to process all computational and programmatic functions. The microcontroller works together with the Power Distribution subsystem to aid in the functions of the Instrument Suite and Communication subsystem components. An inter-integrated circuit (I2C) communication protocol is used to communicate with the microcontroller from the Instrument Suite subsystem, which relays distance information (in centimeters) from scanned points. Subsequently, the data is used for point cloud generation. The sensors within the Instrument Suite subsystem have an internal pull-up pin, which can be used to alternate power between the LiDAR sensors to identify which sensor the telemetry was received from. The microcontroller writes angular measurements to the servomotor for positioning. Every measurement at every increment is packaged and transmitted via ISM radio bands to communicate directly to another device. The transmitter sends data using a 2.4 Ghz frequency range reserved for amateur satellite service. In practice, the transmitter would communicate to the lunar module's receiver. The information received can then be transmitted to the LRO to be relayed for processing through the NASA DSN.

	Mass (kg)	**Volume (mm)**	**Max Power Draw (Wh)**
SG90SR servomotor (theta)	0.009	$22.2 \times 11.8 \times 31$	3.5
MG90 (omega)	0.0134	$32.5 \times 12 \times 35.5$	1.05
Arduino Mega 2560 Rev3	0.037	102×53.3	0.25 (per pin)

Table 4: Technical specifications for C&DH subsystem components: (6) (7) (8)

Modeling

The pseudocode below models a depiction of the point cloud expected to be generated from data received from the device. Algorithm-1 mathematically models the perimeter constraints of the device, adhering to the limitations imposed by its two-degree-of-freedom mechanical architecture. A spherical perimeter bounds the readings, and the results can be interpreted to understand what regions in an environment the instrument can reach. Algorithm-1 adheres to the procedure described in the mechanical subsystem section.

Algorithm 1: Generates mock distance measurements for modeling

$N_x \leftarrow 1000$
Function `GetMockDistances(`N_x`)`**:**
  return 1000 uniform sample distribution x from $0 \rightarrow 2000$ (meters)

Algorithm 2: Registers coordinates using mock distance measurements

$x \leftarrow i$ measurement from N_x
$\omega \leftarrow$ current Algorithm 3 ω
$\theta \leftarrow$ current Algorithm 3 θ
Function `RegisterCoordinates(`x, ω, θ`)`**:**
  x_coordinate $\leftarrow$x $\times \sin\theta$
  y_coordinate $\leftarrow$x $\times \sin\omega$
  z_coordinate $\leftarrow$x $\times \cos\theta$
  return array[x_coordinate, y_coordinate, z_coordinate]

Algorithm 3: Runs mathematical simulation of ATAR spherical perimeter bounds

$A_i \leftarrow$ angular increments
N_ω(yaw) $\leftarrow$ total number of yaw slices
N_θ(pitch) $\leftarrow$ total number of pitch slices
Function `Simulate(`A_i, N_ω, N_θ`)`**:**
  coordinates $\leftarrow$ DataFrame columns[x,y,z,ω, θ]
  increment_value $\leftarrow$ $(\mathrm{A}_i \times \pi)/(180)$
  $\omega \leftarrow$0
  for $i \leftarrow N_\omega$ **do**
    ω += increment _value
    $\theta \leftarrow$-$\pi \times 180$
    x_distances $\leftarrow$ GetMockDistances(N_x)
    for $j \leftarrow N_\theta$ **do**
      append RegisterCoordinates(x_distances[j], ω, θ) to coordinates
      $\underline{\theta}$ += increment_value
  return coordinates

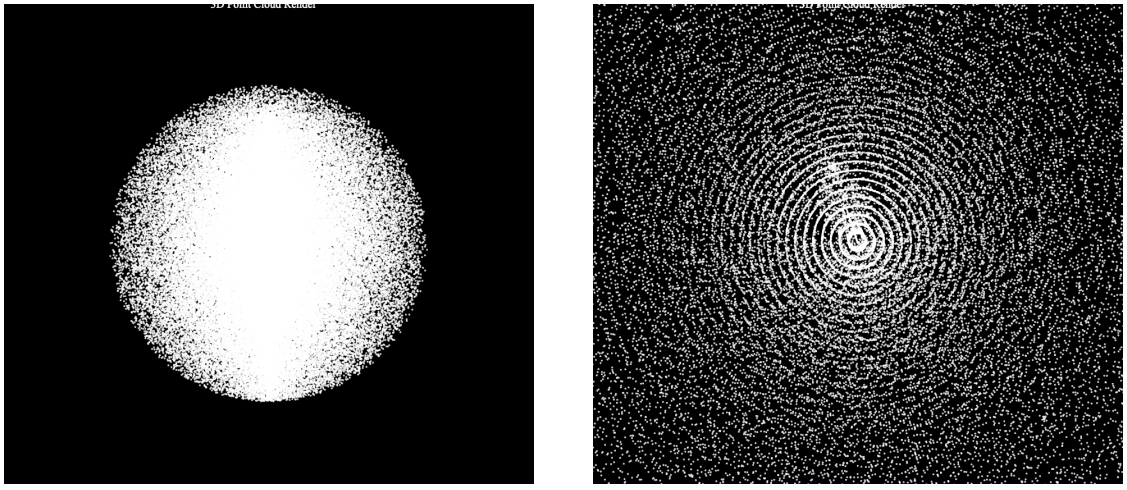

(a) Exterior of the point cloud (b) Interior of the point cloud

Figure 6: Plot of the generated point cloud model of ATAR's spherical perimeter bounds

Figure 6 shows the visual results of the modeling process. LiDAR measurements are recorded and can then be used to find the variables x, y, and z in Algorithm 1. The found coordinates can be converted from spherical to Cartesian coordinates for a point cloud visualization of the deployed site.

Data Analysis

The mechanical system of the device, which houses the servomotors was found to actuate at very low speeds. Due to the weight of the LiDAR sensors and a weak mechanical structure (11), the system struggled to maintain adequate performance under heavy loads. The slow rotation of the servomotors, paired with misaligned angular measurements, results in inaccurate graphical visualizations.

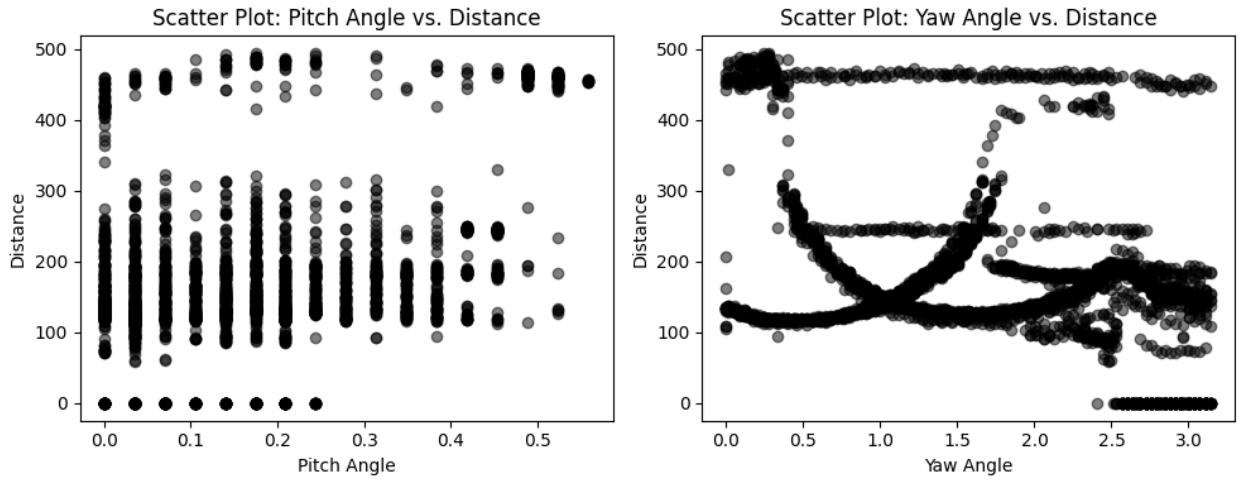

Figure 7: Scatter plot illustrating the relationship between pitch and yaw angles against measured distances during ATAR field testing

Plotting distance measurements derived from the original spherical-to-Cartesian equations alongside angle measurements reveals discrepancies in the collected data.

$x \sin\theta$	$x \sin\omega$	$x \cos\theta$
x-coordinate	y-coordinate	z-coordinate

Figure 8: Spherical-to-Cartesian equations used for point cloud visualization

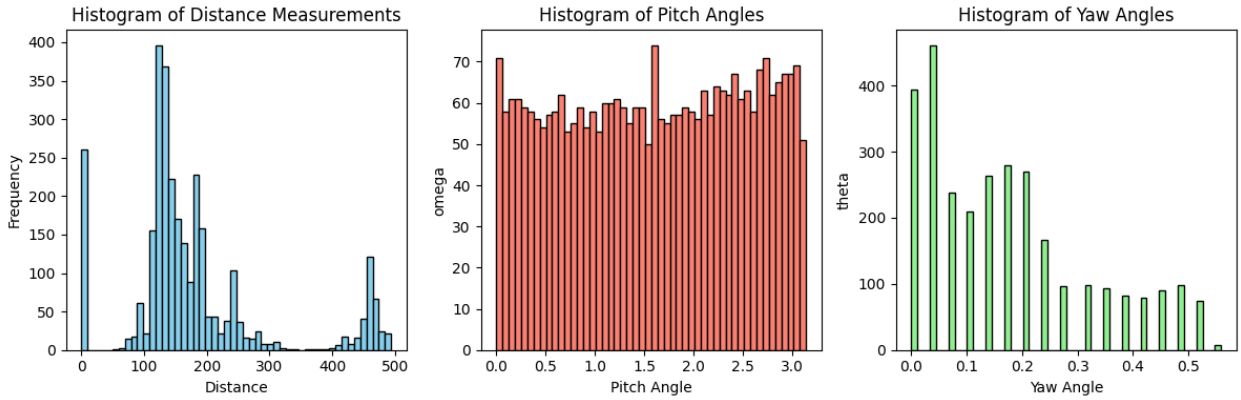

Figure 9: Histogram depicting distances, pitch angle (ω), and yaw angle (θ) observed during ATAR field testing

Field depth can be accurately observed with the collected data, although point cloud rendering cannot, highlighting an important relationship between angular measurements and distance measurements. The device's mechanical structure is prone to error due to terrain and mechanical structure imbalances. The origin point of the servomotors is variable, despite efforts to keep it consistent via software. The servomotor's starting position is variable from the programmed origin. Efforts to keep the origin consistent via software show that heavy loads on small-torque servomotors significantly influence the accuracy of angular measurements. It is critical to emphasize the importance of terrain selection, as selecting dynamic terrains as landing sites will yield significant discrepancies in angular measurements from those of flat terrain. The information concluded from these batch collections of data depicts the importance of precise angular measurements for autonomous vehicles expected to traverse the lunar terrain. The increasing deployment of rovers on celestial bodies, along with tight budget constraints, highlights the need for research in order to minimize error.

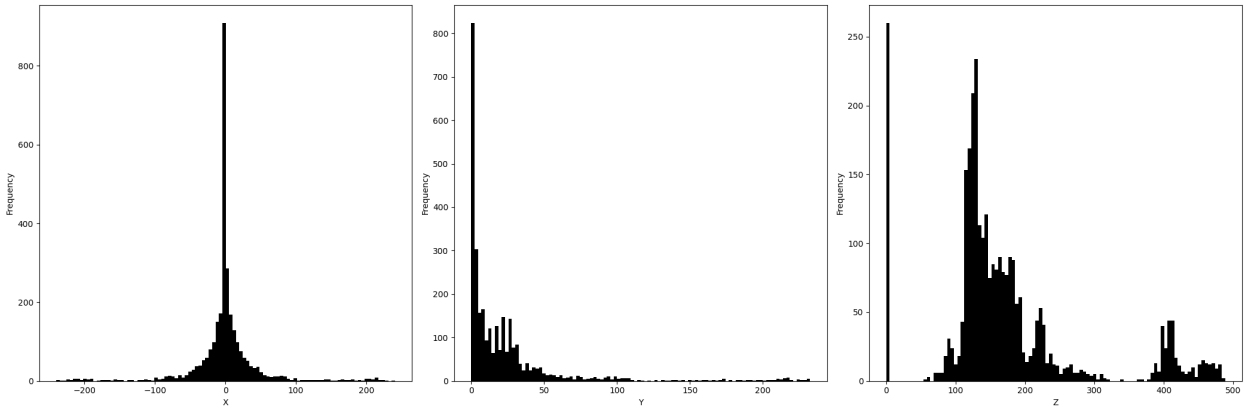

Figure 10: Histogram of x ,y, and z coordinates observed during ATAR field testing

Programmatics

The research group was split into two departments, covering engineering and project management. All workloads for the respective departments were evenly split across the teams as members cross-collaborated in their work. The Project Management (PM) team was responsible for scheduling meetings, organizing operations, and keeping track of milestone dates. Group meeting times accommodated the schedules of members in order to meet project deadlines. Risk management was incorporated into the decision-making process through a consultative and democratic approach to align with the team's objectives. Project direct costs reflected the mission objectives, and purchases were based off of the projected budget plan—additional purchases were made as needed. The group consulted with the faculty leads prior to making a purchase.

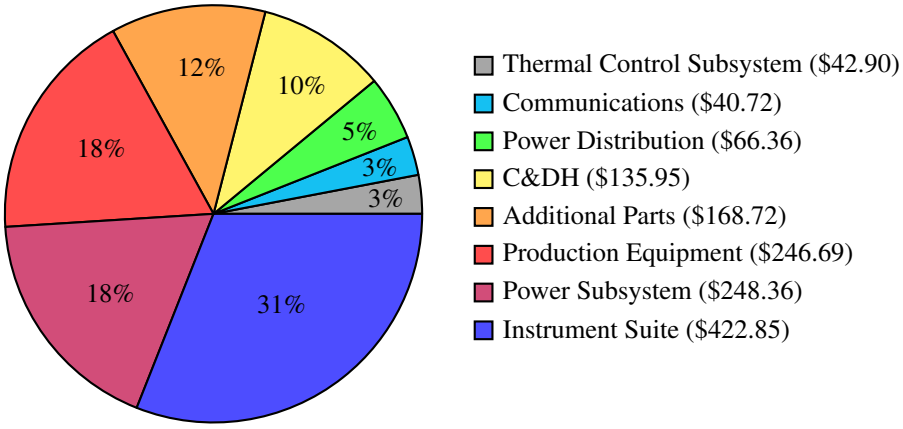

Figure 11: Pie chart showcasing the cost breakdown across all subsystems, including Thermal Control Subsystem (TCS), Communications (Comm), Power Distribution, Command and Data Handling (C&DH), Instrument Suite, Power Subsystem, Additional parts, and Production equipment

Projected Expected Budget	$1,507.12
Projected Actual Budget	$1,372.55
CER Mission Costs (Manufacturing + Wraps)	$5,100,000

Table 5: Table illustrating the projected budget for the ATAR system, presenting expected and actual expenses, alongside conceptual CER mission costs encompassing manufacturing and wrap expenditures

Field Testing Demonstration

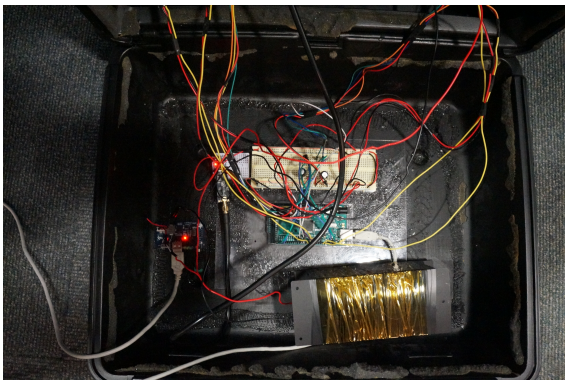

Figure 12: Interior Isometric View

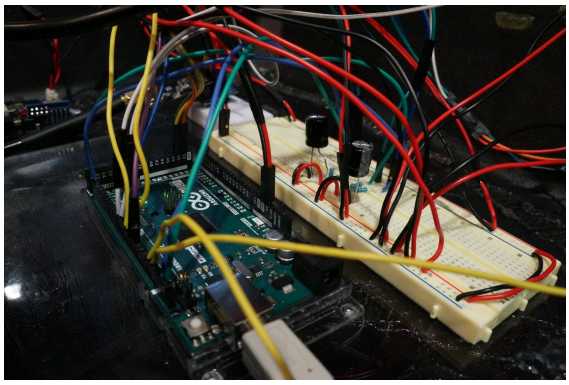

Figure 13: C&DH, Power Distribution and Comm

Figure 14: Indoor field deployment of ATAR

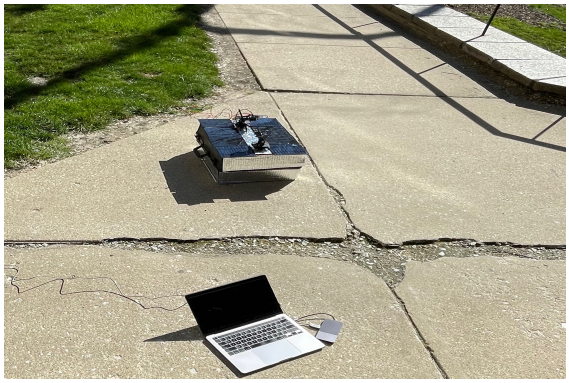

Figure 15: Outdoor field deployment of ATAR

The ATAR device underwent field testing at the Dominican University campus in both indoor and outdoor enviornments (Figure 15). Figures 12, 13, 14 showcase all of the subsystems of the device, accompanied by detailed close-ups of subsystem subassemblies.

Conclusion

Searching for water ice in celestial objects beyond planet Earth presents challenging obstacles to overcome. Settlements on Mars require complex mission planning. However, the use of the Moon as a refueling and restocking station may ease the process. The Apollo missions established fundamental knowledge about the Moon while also disproving other theories. Advancements in modern technology have facilitated regular deployments of landers to the lunar surface. Apollo demonstrated the challenges associated with in-situ experiments conducted by astronauts on the Moon and emphasized the need for autonomous science. Lunar colonization presents challenges to engineers and scientists in habitat and vehicle development. Deploying multiple instances of ATAR across POIs would establish a telemetry-harvesting network of information to assist with manned expeditions to the Moon.

Acknowledgements

The Dominican University ATAR research project is funded by the Guardians of Honor organization through NASA. The STARS research group would like to thank Daniel Rodriguez from Northern Illinois University for his valuable contributions in electrical engineering to ATAR. Dr. Joseph Sagerer aided in addressing project inquiries regarding radiation physics. Credit is given to the NASA L'SPACE Academy for enhancing the skills of project lead Pablo C. Bedolla Ortiz, thereby contributing to the proficiency required for writing this paper.

Budget

Materials	**Cost**	**Quantity**	**Total Cost**
6V 3.5W Solar Panels	$14.50	8	$128.47
Waveshare solar power manager (B)	$30.29	1	$33.55
MOLICEL/NPE 4200mAh flat top lithium-ion battery	$4.85	13	$71.40
Arduino mega 2560 Rev3	$48.40	2	$107.22
HiLetgo 2pc 5V one channel relay module switch with OPTO isolation High-Low level trigger	$7.39	1	$7.39
LIDAR-Lite v3HP	$149.99	2	$318.72
BANRIA 12V 7W flexible polyamide Kapton heater (6 Pack)	$19.89	1	$21.99
HiLetgo DC 3-5V module thermocouple	$7.69	1	$8.52
High voltage boost converter DC-AC 12V Inverter boost board transformer	$10.55	1	$18.67
nRF24LO1+ module + Wireless transceiver module with antenna	$14.99	1	$16.60
ELEGOO breadboard jumper ribbon cable kit	$6.98	1	$7.73
SMA male to SMA female coaxial cables	$10.89	2	$24.12
US energy products (3MM reflective foam insulation shield)	$18.88	1	$20.91
HATCHBOX 1.75mm white PLA 3D printer filament	$24.99	3	$83.04
Creality K1 3D Printer	$579.00	1	$638.00
TOTAL			$1507.12

Table 6: Projected expected budget encompassing all ATAR components, including manufacturing and wrap expenditures

Materials	Cost	Quantity	Total Cost
6V 3.5W Solar Panels	$14.50	8	$128.47
Waveshare solar power manager	$30.29	1	$33.55
MOLICEL/NPE 4200mAh flat top lithium-ion battery	$4.85	13	$71.40
Arduino mega 2560 Rev3	$48.40	2	$107.22
HiLetgo 2pc 5V one channel relay module switch with OPTO isolation High-Low level trigger	$7.39	1	$7.39
LIDAR-Lite v3HP	$149.99	2	$318.72
BANRIA 12V 7W flexible polyamide Kapton heater (6 Pack)	$19.86	1	$21.99
HiLetgo DC 3-5V module thermocouple	$7.69	1	$8.52
High voltage boost converter DC-AC 12V Inverter boost board transformer	$10.55	1	$18.67
Wireless transceiver module with antenna	$14.99	1	$16.60
ELEGOO breadboard jumper ribbon cable kit	$6.98	1	$7.73
SMA male to SMA female coaxial cables	$10.89	2	$24.12
US energy products (3MM reflective foam insulation shield)	$18.88	1	$20.91
HATCHBOX 1.75mm white PLA 3D printer filament	$24.99	3	$83.04
Shurtech Electrical Tape .75X66FT	$3.99	1	$4.82
LEO Sales Plastic Gear Servo - 180	$13.95	2	$28.73
ISPG 1/4 Watt 1% Resitor 610PK	$9.99	1	$10.82
NTE Elect 25V 680UF 105C 2 PK	$1.99	1	$2.82
Jameco Valuepro Breadboard	$11.05	2	$25.85
YIHUA 982-III Precision Soldering Station Kit	$99.99	1	$103.74
HTM-201 Black Silicone Repair Mat Heat Resistant Electronic Repair Mat for Soldering	$11.80	1	$15.55
Soldering Helping Hands	$49.95	1	$53.70
8 AWG Gauge Silicone Wire Electrical Cable (10ft red & 10ft Black)	$19.99	1	$23.74
Elegoo High Temp Tape	$9.99	1	$14.14
TUOFENG 22 AWG Wire Solid Core	$14.99	1	$19.14
20 Pc UXCELL Battery Contact Plates	$10.79	1	$14.94
LK COKOINO Robot Arm for Arduino	$49.99	1	$49.99
SD USA Polyester Hand Held Flag	$2.48	1	$2.48
MKE 12 inch High Tension Hacksaw	$21.97	1	$21.97
Polycarbonate Lexan	$13.96	1	$13.96
Black Bulk Marker	$0.98	1	$0.98
White Paint Marker	$5.97	1	$5.97
Sandnet 120G 10PK	$9.97	1	$9.97
Clear Gorilla Glue	$18.56	2	$37.12
TOTAL			$1372.55

Table 7: Actual budget encompassing all ATAR components, including manufacturing and wrap expenditures

References

[1] National Academies of Sciences, Engineering, and Medicine. *Origins, Worlds, and Life: A Decadal Strategy for Planetary Science and Astrobiology 2023-2032*. The National Academies Press, 2023.

[2] Rutuja Athavale et al. Low cost solution for 3D mapping of environment using 1D LIDAR for autonomous navigation. In *Proceedings of the IOP Conference Seires: Materials Science and Engineering*. 2019.

[3] Gaetano Quattrocchi et al. The thermal control system of NASA's Curiosity rover: a case study. In *Proceedings of the IOP Conference Seires: Materials Science and Engineering*. 2022.

[4] P. Gläser et al. Temperatures near the lunar poles and their correlation with hydrogen predicted by LEND. *Journal of Geophysical Research: Planets*, 2021.

[5] Garmin Support Center. *Lidar-Lite V3HP Operation Manual and Technical Specifications*. 2018. https://cdn.sparkfun.com/assets/9/a/6/a/d/LIDAR_Lite_v3HP_Operation_Manual_and_Technical_Specifications.pdf

[6] Imperial College London. *Servo Motor SG90 Data Sheet*. 2017. http://www.ee.ic.ac.uk/pcheung/teaching/DE1_EE/stores/sg90_datasheet.pdf

[7] Components101. *MG90S – Metal Gear Micro Servo Motor*. 2019. https://components101.com/motors/mg90s-metal-gear-servo-motor

[8] Arduino S.R.L. *Arduino® MEGA 2560 Rev3*. 2023. https://docs.arduino.cc/resources/datasheets/A000067-datasheet.pdf

[9] Molicel. *LITHIUM-ION RECHARGEABLE BATTERY PRODUCT DATA SHEET MODEL INR-21700-P42A*. 2024. https://cdn.shopify.com/s/files/1/0697/3395/files/INR21700P42A-V3-80092.pdf?2425

[10] Arduino. *6 Volt 3.5 Watt Solar Panel*. 2024. https://store-usa.arduino.cc/products/6-volt-3-5-watt-solar-panel

[11] Cokoino and Mosiwi, CKK0006, (2024), Cokoino, https://github.com/Cokoino/CKK0006